Journal of Hydraulic Structures
***J. Hydraul. Struct.*, 2019; 5(1): 60-74**
DOI: 10.22055/jhs.2019.29546.1109

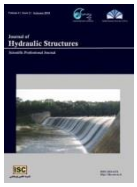

Exploring accuracy of statistical characterization of gravel beds using Kinect device in the laboratory scale

Hadi Bali[1]
Seyed Hossein Mohajeri[2]
Amir Samadi[3]
Maysam Fazeli[4]

Abstract

Mountainous river beds generally consist of gravel particles that the precise description of such bed is not only important hydraulically, but also it has great environmental significance. The accurate estimation of bed roughness gives us valuable information to make reliable hydraulic models of flow in river with rigorous bed form. This study focuses on the accuracy of the Kinect device in determining the digital elevation model (DEM) of the gravel-bed. In this regard, the DEMs of two beds include hemispheres and two beds with artificial gravel beds have been used and their statistical characteristics have been analyzed. The results show that while the error in the area among the particles is quite high, the method can accurately conduct these in general. The comparison of the bed elevation histograms shows that although the artificial gravel beds histograms have higher accuracy compared to the histograms of the beds with hemispheres form, the gravel bed with distance elevations histogram shows the best fit among the four explored beds. Furthermore, exploring the statistical characteristics of these four beds show that the Kinect device is able to obtain reasonable error rate in statistical parameters except the skewness quantity which has the highest rate of relative error. The variogram analysis of artificial gravel beds emphasis that the Kinect and scanner variograms reasonably close to each other and the longitudinal and transversal particles length scales are exactly the same. According to the results of this investigation, application of the Kinect device in statistical analysis of the gravel beds can be suggested.

Keywords: Gravel-bed, Statistical Analysis, Geomorphology, Kinect, Bed Roughness.

Received: 15 May 2019; Accepted: 30 June 2019

[1] Department of Civil, arts and architecture, Islamic Azad University-Science and Research Branch, Tehran, Iran, hadi-bali@hotmail.com.
[2] Department of Civil Engineering, Faculty of Engineering, Kharazmi University, Tehran, Iran, hossein.mohajeri@gmail.com.
[3] Department of Water Sciences and Engineering, Faculty of Agriculture and Natural Resources, Imam Khomeini International University, Qazvin, Iran, amsamadi@gmail.com **(Corresponding author)**.
[4] Department of Civil, arts and architecture, Islamic Azad University-Science and Research Branch, Tehran, Iran, maysam.fazeli57@gmail.com.

1. Introduction

Rivers are significant freshwater sources which have been play an important role in human life. Human demands to water is the main cause of civilizations settlement near the river banks [1]. This consideration is due to human dependence to the water and its considerable effects in different contexts such as agriculture, water transfer and flood control. The first activities regarding to rivers effects in human life, which is somehow within the scope of river engineering practice, is the emergence and growth of civilized societies on the margins of rivers and sustained water resources.

River engineering studies require appropriate river bed roughness characterization to make hydraulic and sediment transport models in order to predict and model the river valleys by numerical modelling methods [2]. For more than a century, the studies regarded to the gravel bed rivers and sediment transport have been done through samples collection from river beds and transferring them to the laboratories in order to sieve them and construct grain size distribution (GSD) curve [3]. The importance of having exact bed particles size refers to the fact that many flow characterizations, such as flow average speed, sediment transport and turbulence features, my affect by rivers bed structure and forms [4] [5]. To measure and determine GSD curve, several methods have been developed such as sieve analysis test (American Material and Testing Association) and image processing methods [6] [7]. Considering the importance of bed roughness, traditional methods which were used to determine aggregates size required huge amount of energy along with low accuracy which make the method not reliable from scientific historical aspects [8] [9].

To overcoming the abovementioned issues, novel methods of determining bed characterizations have been developed as a random field approach [10] [11]. In the new approach, it could be feasible to determine the statistical characterizations of gravel beds by determining digital elevation model (DEM) of the different type of natural to estimate the bed roughness [12]. The statistical characterizations include a vast domain of data such as average bed elevation, bed elevation standard deviation, fractal features and geo-spatial characterizations in small scale [13] [14]. The fundamental step in this approach is to create Digital DEM and point clouds of the bed using different developed methods such as using laser scanner [15], point gauge and Doppler acoustic velocimeter. For more convenience, new methods to make DEM and points cloud have been extended such as photogrammetry techniques [16] [17] like structure from motion (SFM) method [18] [19] [20]. However, scientists are still work on the new techniques to innovate more accurate and convenient methods in this regard.

To determine roughness in the random field approach, number of techniques have been developed. The main purpose of this study is developing new and accurate technique to receive gravel bed parameters using Kinect as an Xbox console. In another words, the main purpose of the study is to quantify the Kinect quality of the constructed DEM of a series of artificial and natural beds through statistical analysis. In this regard, we have done experiments in laboratory scale which will be introduced in the next sections.

2. Experimental procedure

The Kinect facility is produced for the first time by Microsoft Company as a game console for Microsoft Xbox. This device could be used as a low-cost short-range high-resolution 3D/4D camera to simulate spatial data (X, Y, Z) in order to create a 3D model of surfaces. The Kinect includes infrared camera, IR emitter and, RGB camera and several microphone arrays to receive environmental sounds. Details of the Kinect device have been illustrated in figure (1). The IR

emitter is capable to determine 3D surfaces by optical networking structure [21]. Experimental results show that the random error of depth measurement increases when the sensor become far from the object. The range of random error changes from 1 mm (at the distance of 500 mm) and 75 mm (at the distance of 5000mm) [22]. The error limitation has enough accuracy for gravel bed studies, but it can be checked through experiments in this study.

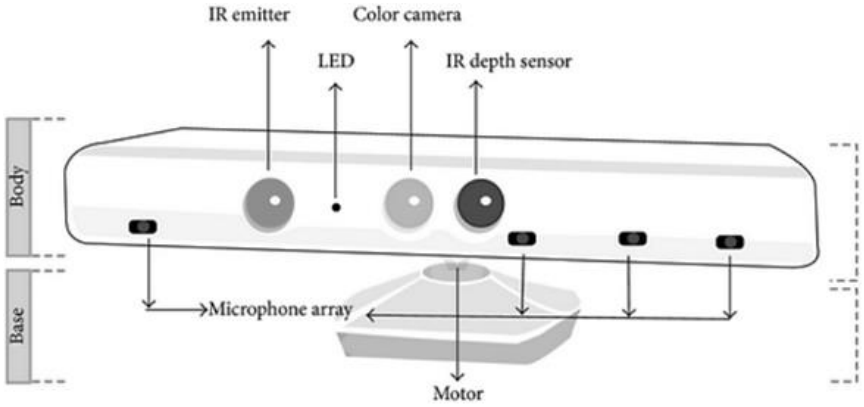

Figure 1. The Kinect device components

In this study, finding the abilities and accuracy of the Kinect - in generating DEM of gravel beds divided in two main steps. At the first step, in order to verify the method, regular shape objects with defined surface equation like hemisphere has been used. For appropriate method verification, two hemispheres with different size of diameters has been selected.

The hemisphere shape has been used for laboratory test because of its similarity to gravel beds particles. Two different diameters and materials with hemispheres shape were built in laboratory which have been shown in figure (2). Smaller hemispheres has 28 mm diameter which is built by cement grout (figure 2-a). Greater hemispheres were created in 60 mm diameter by a 3D printer with FDM technology (figure 2-b). The color of cement grout (gray) is the same as gravels color and therefore we have color reassembly between men make hemisphere and natural gravel. To make the hemispheres surface smoother, they have been polished by a very soft sand paper and then painted by the spray. It causes the reduction in errors of Kinect's 3D model.

a) **b)**

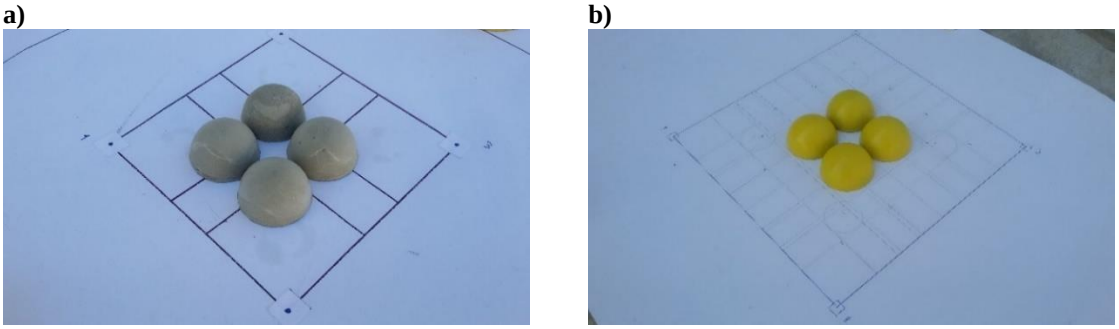

Figure 2.Beds which consist of hemisphere shaped objects: a) Small cement hemispheres, b) large plastic hemispheres

The 3D surface of beds (4 hemisphere) has been detected by Kinect and Skanect software. A scaled paper has been drawn in AutoCAD to set as a background. It helps us to scale the data from Kinect spatial outputs to Cartesian DEM coordinates.

In second step, random size natural gravels (which were collected from a natural river bed) have been glued on a plate to simulate the river bed artificially in laboratory. The plate made of wood with 400×400 mm length. Simulated river beds have two major types which is depicted in figure (3). Simulated river bed includes 1) collection of grains with no space and 2) collection of grains with considerable space.

a) **b)**

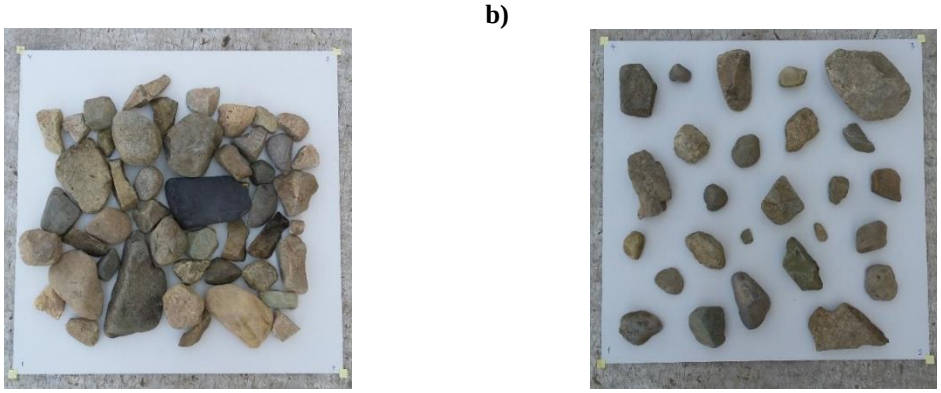

Figure 3. Artificial simulated gravel beds: a) Simulated gravel bed - collection of grains with no space, b) Simulated gravel bed collection of grains with considerable space

The simulated river bed has a great degree of irregularity in space. This makes the verifying process of the real bed with generated bed by Kinect so hard. For verifying process, the MATLAB code has been developed to calculate the special error between real bed height and generated bed by Kinect. In case of simulated gravel beds, high resolution DEM is necessary to generate high density point clouds with the minor errors as a pattern to compare- with DEMs generated by Kinect. 3D scanners can help us to catch the real bed DEM as an accurate and reliable device. In this study, a Solutionix C500 (new generation of 3D scanner) was used where this facility is shown in figure (4). The Solutionix C500 is an industrial 3D scanner, which released in 2017 by MEDIT Metrology Engineering Group for the first time, optimized for the automatic scanning of small to medium objects. Dual 5.0MP cameras -prepares high resolution facilitate to capture 3D components, where the accuracy is limited down to a few microns (50 micron). The device covers four visibilities with 9, 175, 350 and 500 mm length for different resolution which is shown in table (1). The C500 is portable and can be placed over an office desk and have very simple usage. Scanning easily and rapidly makes it more user-friendly, and also automatic turntable with 10 Kg weight capacity, convince us to use Solutionix C500 in this study. This scanner generates DEM in STL format using ezScan 2017 software [23].

The Kinect equips Infrared technology, and this system make it inappropriate for utilizing in daylight. Interfering sunlight and Kinect infrared ray causes considerable noises in results in field surveys on day. Because of this, Kinect can be applied in laboratory under controlled condition, to obtain accurate results. The experiment starts by setting up the Kinect - and link it to the Skanect software. We can circulate the kinect around the objects in different angle and simultaneously the point clouds are generating by Skanect software in PLY formant. At the end of data acquisition, the raw data need to be edited or corrected where MeshLab software has been utilized.

Figure 4.The used 3D scanner (Solutionix C500)

Table 1. Solutionix C500 characterizations in four visibility

VISIBILITY	SCANNING VOL. (MM)	RESOLUTION (MM)
90MM	68 × 56 × 30	0.028
175MM	136 × 111 × 60	0.056
350MM	264 × 218 × 120	0.110
500MM	385 × 312 × 210	0.157

In second step, generated 3D DEM were sent to the MATLAB code to extract special parameters. This process was conducted for regular defined bed (hemisphere) and irregular random bed (collected grain with and without space). In regular defined bed, the height of DEM in exactly determined by hemisphere mathematical equation but in irregular random bed, we must use 3D scanner to generate accurate DEM which is introduced as a real data. Difference between Kinect spatial DEM data and real bed form can lead to calculate mean relative errors, absolute mean errors, standard deviation and skewness of the DEM height. Analysis and results of statistical extracted parameters in following section has been described in next section.

3. Results

In this study, the digital elevation model of different beds forms has been made and then statistical parameters have been computed by various open source codes in MATLAB. The results can present in two main categories which is coincident to the type of bed forms. As mentioned before, these two types are regular defined bed and irregular random bed. The absolute mean error and relative mean error are two main parameters which are used to evaluate the accuracy of Kinect output in new DEM generation technique. The equations as below:

$$AMnError = Z_{kinect} - Z_{real} \quad (1)$$

$$RMnError = \frac{AMnError}{Z_{real}} \times 100 \quad (2)$$

Where Z_{kinect} is the DEM elevation using Kinect and Z_{real} is the bed real elevation.

3.1. The regular defined objects (hemispheres) models

Figure (5-a) shows the DEM generated by the Kinect - for the bed consist of four hemispheres with 28 mm diameters. The absolute difference between Kinect DEM acquisition and real bed can be seen in figure (5-b). Obviously, absolute differences which are equivalent to

simulation errors are increased in the zone between hemispheres due to hemisphere shading. It means that the IR rays could not detect the narrow and deep areas between the bed objects. On the contrary, the upper part of surface where the IR ray reach it directly shows less error. Some main statistical parameters like absolute mean error, relative mean error and Standard deviation of error has been presented in table (2). The absolute mean error is 1.5 mm where it is smaller than 28mm (hemisphere diameters) and show that the mean error (1.5 mm) is much little in comparison to the diameters of the hemispheres.

a)

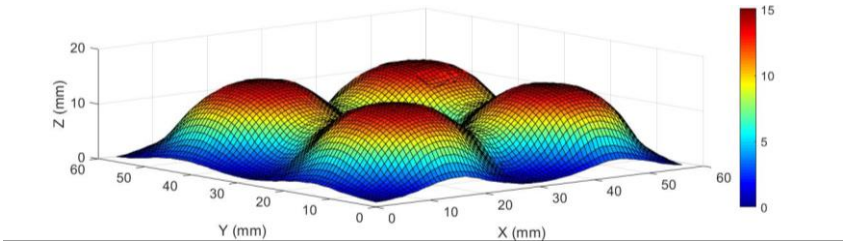

b)

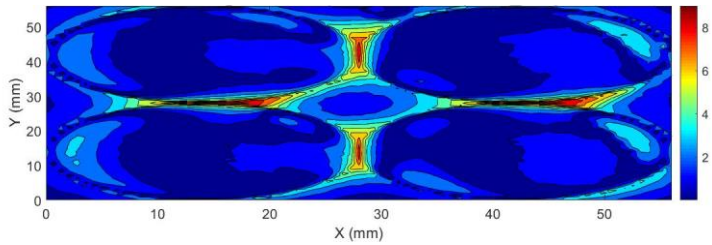

Figure 5. Analysis of the bed with hemispheres (28mm diameter): a) The DEM created by Kinect device, b) Difference of the Kinect output with hemisphere mathematical equation.

Table 2. Statistical parameters of the bed consist of small hemispheres.

Statistical Parameter	Absolute Mean Error (mm)	Relative Mean Error (%)	Standard Deviation of Errors (mm)
Amount	1.59	22.25	1.39

The previous experiment has been repeated for greater hemispheres (60mm diameter) (as shown in figure (2-b)) to check the effect of hemisphere size in statistical parameters and errors. The results are shown in figure (6) and table (3). The main results are the greater diameters the greater Absolute mean error but the less relative mean error.

a)

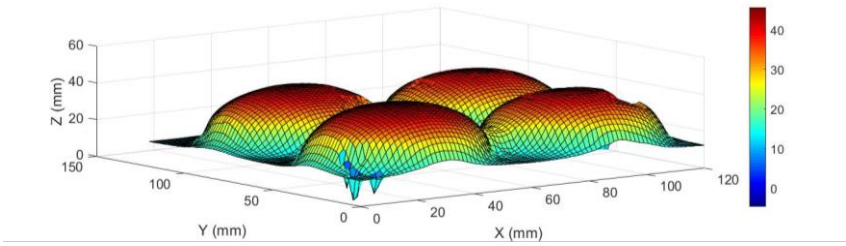

b)

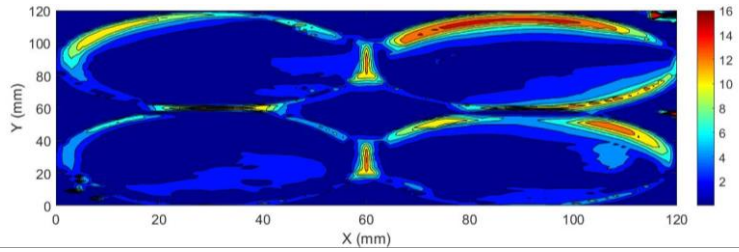

Figure 6.Analysis of the bed with hemisphere (60 mm diameter): a) The DEM created by Kinect , b) Difference of the Kinect output with hemisphere mathematical equation

Table 3. Statistical parameters of the bed consist of large hemispheres

Statistical Parameter	Absolute Mean Error (mm)	Relative Mean Error (%)	Standard Deviation of Errors (mm)
Amount	2.58	16.87	2.91

3.2. The Irregular random bed

In this section, the Kinect output performance is checked and evaluated for simulated gravel bed. Two types of simulated gravel beds are introduced before:

1) Simulated gravel bed collection of grains with no space.

2) Simulated gravel bed- collection of grains with considerable space.

Figure (7-a) shows the DEM generated by Kinect for the simulated gravel bed collection of grains with no space. As it mentioned in the previous sections, automatic 3D scanner has been utilized to generate 3D DEM of simulated gravel bed. The DEM which created by 3D scanner is shown in figure (7-b). By subtracting the two DEMs in MATLAB, the difference between them has been appeared as it is shown in figure (7-c). The results show that errors are increasing rapidly at the peak of the grains where the sharp changes at the edges are presence. Table (4) shows the statistical parameters calculated by MATLAB code for this type of bed.

a)

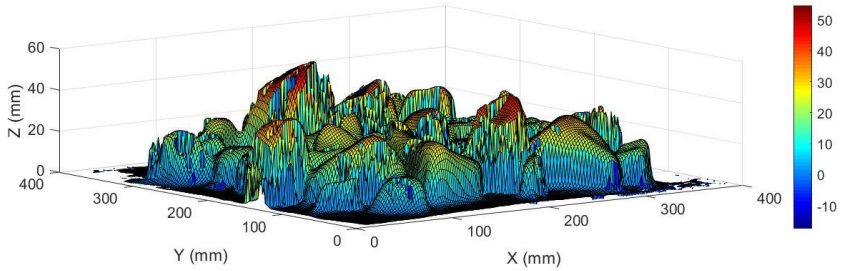

b)

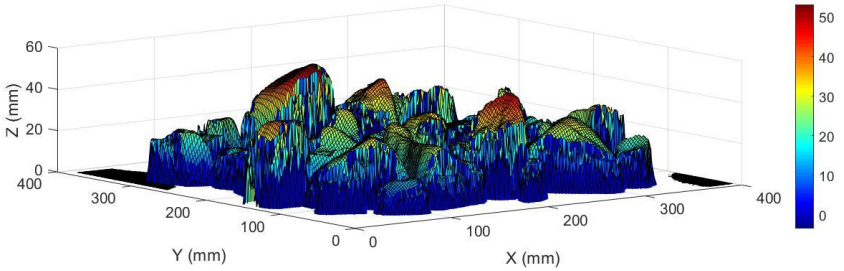

c)

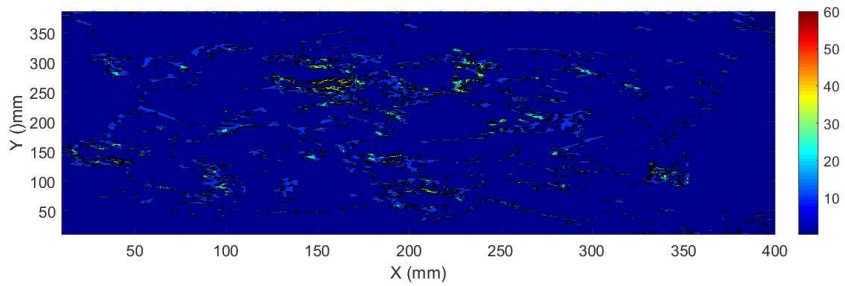

Figure 7. Analysis of the simulated gravel bed with no space: a) The DEM created by Kinect, b) The DEM created by Solutionix C500 3D scanner, c) The difference between two Dems.

Table 4. Statistical parameters of the simulated gravel bed with no space.

Statistical Parameter	Absolute Mean Error (mm)	Relative Mean Error (%)	Standard Deviation of Errors (mm)
Amount	3.92	85.19	5.84

For Another type of bed with collection of grains with considerable space, the same analysis has been done. Figure (8-a and b) shows the DEMs has been created by Kinect and 3D scanner respectively. By subtracting two DEMs, the difference of them has been appeared as it shown in figure (8-c). The figure shows that errors are increased at the sharp changes at the edges. The statistical parameters are shown in table (5).

a)

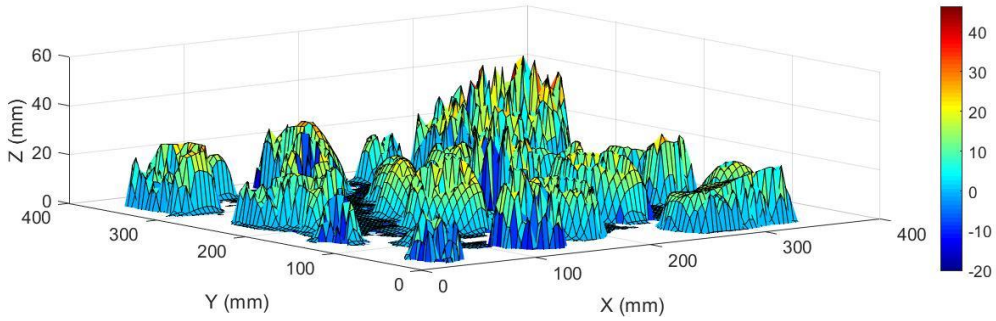

b)

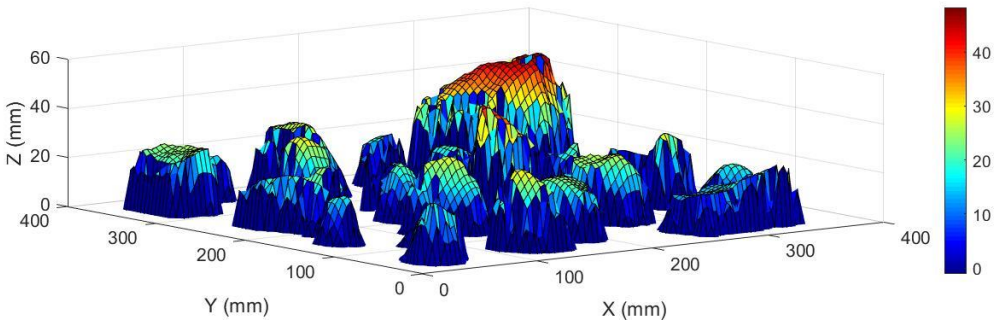

c)

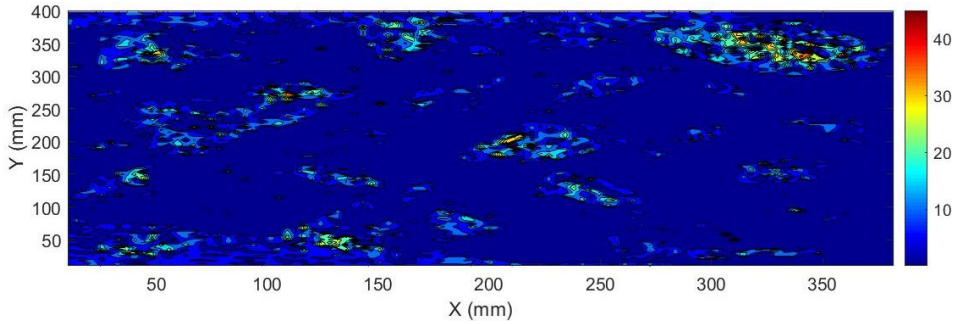

Figure 8. Analysis of the simulated gravel bed with distance arrangement: a) The DEM created by Kinect device, b) The DEM created by Solutionix C500 3D scanner, c) The difference between two DEMs

Table 5. Statistical parameters of the simulated gravel bed with distance arrangement

Statistical Parameter	Absolute Mean Error (mm)	Relative Mean Error (%)	Standard Deviation of Errors (mm)
Amount	3.94	37.56	5.66

Figures (9-a) and (9-b) show the pie chart for comparing the absolute mean error and relative mean error in four explored beds. According to the charts, while the absolute mean error of the bed consists of small hemispheres is less than that of large hemispheres, the relative mean error of the bed consist of small hemispheres is higher than the bed with large hemispheres. It is because of the increase of the bed objects size in the second bed. The same figure is happened in simulated gravel beds as the relative mean error of the simulated gravel bed with distance arrangement experienced an increase of more than twice as much as the figure for the gravel bed with no distance arrangement while the absolute error of the both beds is nearly equal. The significant increase in relative mean error of the bed with no distance arrangement, refers to the relative error equation as it mentioned in Eq. (2). In fact, the distances between bed aggregates results to have less amounted theoretical elevation (Z_{theo}) which lead to have higher amounts for relative mean errors in this case.

a) **b)**

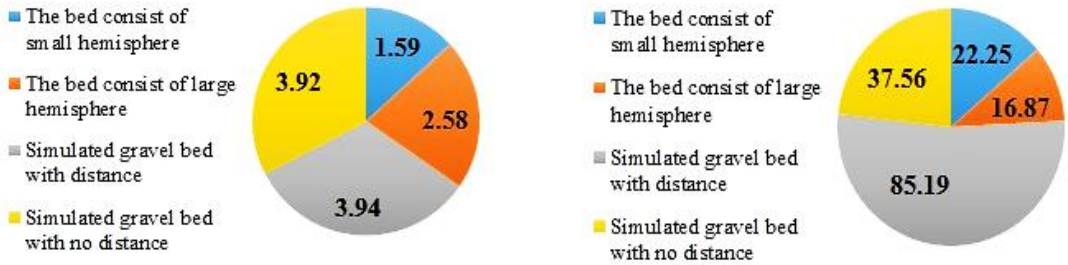

Figure 9. The comparison between four bed errors: a) Absolute mean error pie chart, b) Relative mean error pie chart

In the statistical analysis of gravel beds, a distribution function is a comprehensive and fundamental parameter [13] [24]. In these statistical parameters such as standard deviation,

skewness and kurtosis can be qualitatively notified through the distribution and histogram. Due to this fact, a clear and high accurate description of this parameter is essential for any technique which is applied in this approach for the first time. To compare the efficiency of Kinect device to make the data distribution, in figure (10) the histograms of the Kinect and the base cases (i.e. theoretical and scanner) elevations in four explored beds are shown. In each subplot, red line refers to Kinect results, while the blue-cross line implies the base cases. This figure shows that the bed elevations histogram of small and large hemispheres (i.e. figure (10-a and b) respectively) using Kinect are drastically different with the base cases. Also, as it is clear, the bed points elevation with small values shows more difference in distribution than the rest of the elevation's histogram. In contrast, the histogram of simulated gravel beds with/without distance, figure (10-c and d), is almost fitted with the constructed bed using 3D scanner. However, the high difference can be observed in figure (10-b, c and d) for small values as figure (10-a, b). Such difference in this area which are referred to the trough areas between the hemispheres shows that the Kinect device between the hemispheres cannot properly construct the DEM between the particles. Deeper analysis shows that, despite the fact that in small values the difference of Kinect and base cases elevations histogram is high, comparison of figure (10-c and d) shows that the histograms of the bed points elevation histogram of the simulated bed consist of gravels with distance, seems to be more fitted. As a result, it could be deducted that although the Kinect device creates more accurate DEM for upper areas of the bed aggregates, its result for the downer areas may have less quality. For such observation three reasons could be speculated. Firstly, the distance between the measured points and the location of the Kinect device. In fact, the distance of particles crest to the location of the Kinect device is generally smaller than that of particles trough to the location of the Kinect. Such difference can be a source of error of the observed difference. Secondly, the existence of the shadow of particles in the trough of the bed. Finally, it could be possible that in the little space between the bed particles less IR rays emits which cannot completely cover this area.

a)

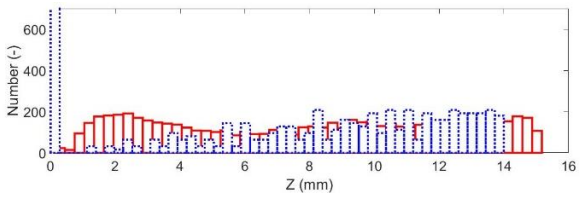

b)

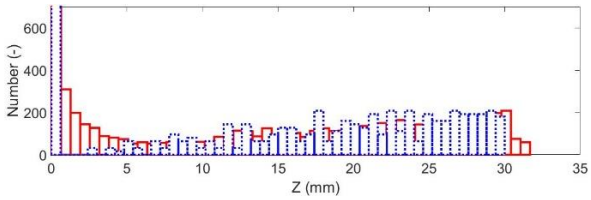

c)

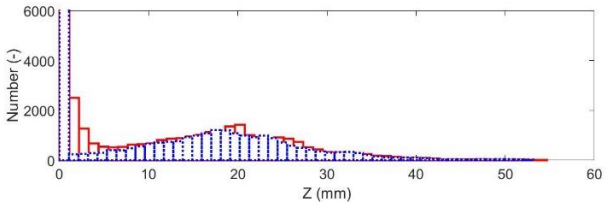

d)

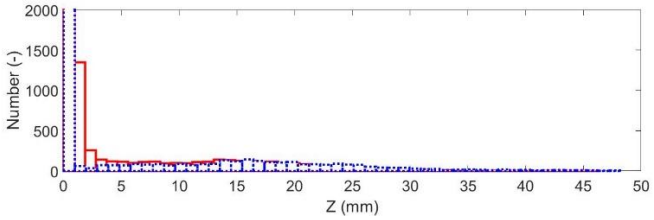

Figure 10. The comparison between Kinect (red-line) and base case (blue-cross line) histograms: a) Small hemispheres, b) Large hemispheres, c) Simulated gravel bed without distance, d) Simulated gravel bed with distance

For further exploring the efficiency of Kinect device in statistical characterization, in table (6) statistical parameters of the DEMs created by Kinect device are compared with those values of the base cases. These statistical parameters are composed of mean, standard deviation, skewness and kurtosis of the bed elevations. Also, some of these values have important physical meaning. As an example, in previous studies it is shown that the standard deviation of elevations of the bed potentially could be considered as the bed roughness coefficient [13] [7]. For better understanding of errors, the amount of relative mean errors is reported which are calculated by Eq. (3):

$$RMErr = \frac{A_{Kinect} - A_{Base\ case}}{A_{Base\ case}} \times 100 \tag{3}$$

Where A could be each of these parameters i.e. the mean, standard deviation, skewness or kurtosis and indices depicts the methods they come from. As it can be seen in Table 6, the skewness error has the highest value among all the calculated errors for all the parameters. Also, among the skewness error, the bed consists of small hemispheres has the largest relative error. While the gravel bed without distance has experienced the lowest rate in relative mean errors, in general, the figures for gravel bed with distance are the highest among four explored beds.

Table 6. Comparison of the statistical parameters of four experimental beds

Beds consist of hemisphere shaped objects

Small hemispheres				Large hemispheres			
Parameter	Real values (mm)	Observed values (mm)	Relative Mean Error (%)	Parameter	Real values (mm)	Observed values (mm)	Relative Mean Error (%)
Mean	8.01	7.14	12.18	Mean	14.96	15.303	2.23
Standard Deviation	4.39	4.91	10.58	Standard Deviation	10.74	10.51	2.13
Skewness	-0.06	-0.33	80.17	Skewness	-0.17	-0.33	49.15
Kurtosis	1.66	1.65	0.69	Kurtosis	1.634	1.65	0.82

Artificial simulated gravel beds

With Distance Gravel Bed				Without Distance Gravel Bed			
Parameter	Real values (mm)	Observed values (mm)	Relative Mean Error (%)	Parameter	Real values (mm)	Observed values (mm)	Relative Mean Error (%)
Mean	3.168	4.603	31.17	Mean	10.999	10.501	4.74
StandardDeviation	8.57	9.67	11.40	Standard Deviation	12.005	11.93	0.63
Skewness	1.11	1.87	40.65	Skewness	0.53	0.79	33.15
Kurtosis	4.76	5.82	18.27	Kurtosis	2.68	2.78	3.69

Additional information on the statistical characterizations of the bed can be extracted from variogram of bed elevations [13] [24]. In fact, variogram is an important parameter in spatial data statistical analysis which has been widely used for characterization of gravel bed rivers. Robert [25] used the variogram in his studies and proved that one-dimensional variogram can be defined as Eq. (4) and (5):

$$D_2\left(l_x\right)=\frac{\sum_{j}^{M}\sum_{i}^{N-n}\left[\left|Z\left(x_i+n\delta x,y_j\right)-Z\left(x_i,y_i\right)\right|\right]^2}{M\left(N-n\right)} \tag{4}$$

$$D_2\left(l_x\right)=\frac{\sum_{j}^{N}\sum_{i}^{M-m}\left[\left|Z\left(x_i,y_j+m\delta y\right)-Z\left(x_i,y_i\right)\right|\right]^2}{N\left(M-m\right)} \tag{5}$$

Where $\Delta x=n\delta x$ and $\Delta y=n\delta y$ are longitudinal and transverse spatial lags, δx and δy are spatial sampling intervals, N and M are the total number of measuring points of bed elevation in direction x and y, respectively. ‖ denotes absolute value, and [] defines averaging over many point pairs. Both longitudinal and transverse variogram reveal the existence of three ranges: scaling, transition, and saturation regions. Characteristic scales (l_x ; l_y) of the gravel bed in the longitudinal and transverse directions can be defined based on $D_2\left(\Delta x\right)$ and $D_2\left(\Delta y\right)$ as spatial lags corresponding to the intersections of the scaling and saturation regions [13] [15]. In this study, the variogram function has been calculated for the two simulated gravel bed without/with distance for both Kinect and 3D scanner data and the results have been compared in both longitudinal and transverse directions as it is shown in figure (11) which the three mentioned regions are observable. The comparison of variograms for Kinect and scanner in gravel bed without distance are shown in the graphs of figures (11-a and b) for longitudinal and transverse directions, respectively, which the hollow circles imply the Kinect results and cross sign show the scanner results. The charts of figures (11-c and d) are shown the same results for simulated gravel bed with distance for longitudinal and transverse directions, respectively. Deeper explores lead to the fact that the variogram has the same treat in both longitudinal and transverse directions in two explored bed. Moreover, the amounts of l_x and l_y in both directions are the same which is align to the results of gravel bed variograms investigations represented by previous studies [13] [24] [26]. As it is shown in the charts of figure (11), the both amounts of l_x and l_y for gravel bed with distance are equal to 2.2 (mm) and for the gravel bed without distance are equal to 2.4 (mm).

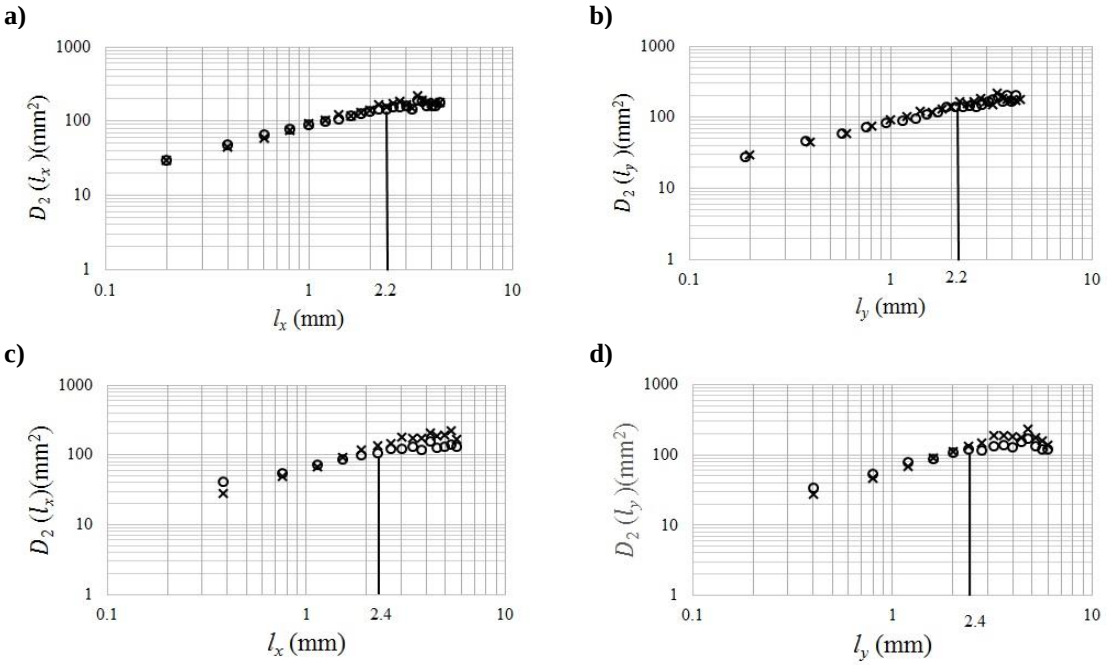

Figure 11. One-dimension variogram of bed elevations for simulated gravel beds: a) Longitudinal directions of Kinect results for gravel bed without distance, b) Transverse direction of Kinect results for gravel bed without distance, c) Longitudinal directions of Kinect results for gravel bed with distance, d) Transverse direction of MATLAB extended results for gravel bed with distance

4. Conclusions

This study explored the applications of the Kinect device in statistical analysis of gravel beds considering random field approach. For this purpose, a set of artificial beds composed of hemispheres and gravel particles are built to control the accuracy of the constructed DEM. The results confirm that the Kinect device gives the possibility of exploring statistical analysis of beds by creating Digital Elevation Model (DEM) of the bed. Analyzing the results of data acquired by the Kinect device shows that it creates DEM accurately, while the area between the particles cannot constructed precisely. The comparison of the bed elevation histograms resulted that although the artificial gravel beds histograms have higher accuracy compared to the histograms of the beds consist of hemispheres, the gravel bed with distance elevation histogram shows the best fit among the four explored beds. Further exploring the statistical characteristics of these four beds show that the Kinect device may result in obtaining reasonable error rate of statistical parameters except of the skewness which has the highest rate of relative error. In addition, analyzing the variogram of artificial gravel beds clarified that the Kinect and scanner variograms reasonably match to each other and the estimated longitudinal and transversal particles length scales are exactly the same. According to this investigation, it can be advised to use the Kinect device in statistical studies of the gravel beds. However, this study explores the ability of Kinect device by artificial gravel beds in laboratory conditions and it suggests for future investigations to explore the Kinect device abilities in statistical analysis of gravel beds of natural rivers.

References

1. Boostani A., Esmaili K., "River engineering, from the past to the future (Evaluationof approaches and outlooks)," Journal of Water and Sustainable Developments, vol. 1, no. 3, pp. 67-72, 2015.
2. Hassannezhad Sharif F., Samadi A., Azizian Ghatar A., "Evaluation of Image Processing Technique in Estimating the Manning's Roughness Coefficient in the Surface Layer of Riverbeds," Iranian Journal of Soil and Water Research, vol. 47, no. 4, pp. 711-722, 2017.
3. Lamarre H. and Roy A. G., "Reach scale variability of turbulent flow characteristics in a gravel-bed river," Geomorphology, Vols. 68, pp. 95-113, 2005.
4. Buffin-Bélanger T., Roy A. G., "Effects of a pebble cluster on the turbulent structure of a depth-limited flow in a gravel-bed river," Geomorphology, 1998.
5. Nikora V., Goring D., McEwan I. and Griffiths G., "Spatially averaged open-channel flow over rough bed," Journal of Hydraulic Engineering, Vols. 127,2, pp. 123-133, 2001.
6. Graham D. J., Reid I. and Rice P., "Automated sizing of coarse-grained sediments: image-processing procedures," Mathematical Geology, vol. 37(1): 28, 2005.
7. Mohajeri SH., Safarzadeh A., Salehi Neyshabouri A., "Determination of the Longitudinal Velocity Profile of Turbulent Flow over Rough Beds Using Double Averaging Method," Journal of Modares Civil Engineering, vol. 18, no. 4, pp. 265-276, 2018.
8. Nikora V. I., Koll k., McEwan I. K., McLean S. R., Dittrich A., "Velocity distribution in the roughness layer of rough-bed flows," Journal of Hydraulic Engineering, Vols. 130(7), pp. 1036-1042, 2004.
9. Nikora V., Mcewan I., Mclean S., Coleman S., Pokrajac D. and Walters R., "Double averaging concept for rough-bed open-channel and overland flows: Theoretical background," Journal of Hydraulic Engineering, Vols. 133, 8, pp. 873-883, 2007.
10. Hemmelder, S., Marra, W., Markies, H., De Jong, SM., "Monitoring river morphology & bank erosion using UAV imagery – A case study of the river Buëch, Hautes-Alpes, France," Journal of Applied Earth Observations & Geoinformation, vol. 73, pp. 428-437, 2018.
11. James, MR., Chandler, JH., Eltner, A., "Guidelines on the use of structure-from-motion photogrammetry in geomorphic research," Earth Surface Processes and Landforms, 2019.
12. Ashmore, P., Leduc, P., Peirce, S., "Short communication: Challenges and applications of structure-from-motion photogrammetry in a physical model of a braided river," Earth Surface Dynamics, vol. 7, pp. 97-106, 2019.
13. Nikora V. I., Goring D. G. and Biggs B. F., "On gravel-bed roughness characterization," Water Resources Research, Vols. 34, pp. 517-527, 1998.
14. Groom, J., Friedrich, H., "Spatial structure of near-bed flow properties at the grain scale," Geomorphology, vol. 327, pp. 14-27, 2019.
15. Mohajeri H., Grizzi S., Righetti M., Romano G. P., Nikora V., "The structure of gravel-bed flow with intermediate submergence: a laboratory study," Journal of Water Resources Research.

16. Bertin, S., Friedrich, H., "Measurement of gravel-bed topography: evaluation study applying statistical roughness analysis," Journal of Hydraulic Engineering, vol. 140, no. 3, pp. 269-279, 2013.
17. Ruther, N., Huber, S., Spiller, S., Abrele, J., "Verifying a photogrammetric method to quantify grain size distribution of developed armor layers," Proceedings of 2013 IAHR Congress, 2013.
18. Micheletti, N., Chandler, J.H., Lane, S.N., "Structure from Motion (SFM) Photogrammetry," BSG, Vols. ISSN 2047-0371, 2015.
19. Fonstad, M.A., Dietrich, J.T., Courville, B.C., Jensen, J.L., Carbonneau, P.E., "Topographic structure from motion: a new development in photogrammetric measurement," Earth Surface Processes and Landforms, vol. 38, no. 4, pp. 421-430, 2013.
20. Westoby, M.J., Brasington, J., Glasser, N.F., Hambrey, M.J.,Reynolds, J.M., "Structure-from-Motion' photogrammetry: a low-cost, effective tool for geoscience applications," Geomorphology, vol. 179, pp. 300-314, 2012.
21. Freedman, B., Shpunt, A., Machline, M., Arieli, Y., "Depth mapping using projected patterns.," Prime Sense Ltd., United States, 2010.
22. Khoshelham K., Sander E., "Accuracy and Resolution of Kinect Depth Data for Indoor Mapping Applications," Sensors, vol. 12, no. 2, p. 1437–1454, 2012.
23. "Solutionix C500," [Online]. Available: https://europac3d.com/3d-scanners/solutionix-c500/).
24. Nikora V., Walsh J., "Water-worked gravel surfaces: High-order structure functions at the particle scale," Water Resource, vol. 40, 2004.
25. R. A., "Fractal properties of simulated bed profiles in coarse-grained channels," Mathematical Geology, vol. 32, no. 3, p. 367–382, 1991.
26. M. S. H., "Hydrodynamics of gravel bed flows (Implications in colmation)," PhD Thesis, Department of Civil, Mechanics and Environmental Engineering, University of Trento and School of Geography, Queen Mary University of London, 2014.
27. James, M.R., Robson, S., "Straightforward reconstruction of 3D surfaces and topography with a camera: Accuracy and geoscience application," Journal of Geophysical Research, 2012.
28. Davis A., Marshak A., Wiscombe W. & Cahalan R., "Multifractal characterizations of nonstationarity and intermittency in geophysical fields: Observed, retrieved, or simulated," Journal of Geophysics, vol. 99, p. 8055–8072, 1994.